

Self-Induced Cyclic Reorganization of Free Bodies through Thermal Convection

Bin Liu (刘斌)^{1,2} and Jun Zhang (张骏)^{1,2,*}

¹Center for Soft Matter Research, Department of Physics, New York University, 4 Washington Place, New York, New York 10003, USA

²Applied Mathematics Laboratory, Courant Institute, New York University, 251 Mercer Street, New York, New York 10012, USA
(Received 30 October 2006; published 16 June 2008)

We investigate the dynamics of a thermally convecting fluid as it interacts with freely moving solid objects. This is a previously unexplored paradigm of interactions between many free bodies mediated by thermal convection, which gives rise to surprising robust oscillations between different large-scale circulations. Once begun, this process repeats cyclically, with the collection of objects (solid spheres) entrained and packed from one side of the convection cell to the other. The cyclic frequency is highest when the spheres occupy about half of the cell bottom and their size coincides with the thickness of the thermal boundary layer. Our work shows that a deformable mass stimulates a thermally convecting fluid into oscillation, a collective behavior that may be found in nature.

DOI: [10.1103/PhysRevLett.100.244501](https://doi.org/10.1103/PhysRevLett.100.244501)

PACS numbers: 47.27.te, 05.65.+b, 47.20.Bp

Over the past 30 years, thermal convection has come to be regarded as a paradigm for the study of dynamical systems [1,2]. Its study has revealed fundamental and generic features of systems driven from equilibrium and into chaos [3,4]. Many important questions remain open, especially regarding heat transport rate at high Rayleigh numbers [5–7] and the formation and dynamical stability of the large-scale circulation [8,9].

To date, most experimental and theoretical works on thermal convection have dealt with fixed boundary conditions: the walls are rigid and hence do not respond to or interact with the changing fluid flows confined within. However, many interesting fluid dynamics problems involve moveable or shape-changing boundaries and walls that interact with time-dependent fluid flows [10]. While many such examples arise in biological physics [11], and are the subject of much intense activity, they also arise in geological physics where thermal convection comes into play.

Experiments on interaction between free boundaries and thermal convection is a mostly unexplored subject. Previous experiments [12–15] simulated a single body, a floating continent, that drifted above and interacted with a “mantle” convecting underneath. The work reported here considers the interaction of many freely moving bodies with a thermally convective fluid. One of our motivations is to begin understanding the interplay of many “microplates,” instead of large continents, that interact with the convective mantle. The system is dynamically rich with, for example, periods of global circulation rearrangement coupled to ordered packing and unpacking of the free bodies.

A fluid, when heated from below and cooled at the top, is subject to buoyancy instability; subsequently, Rayleigh-Bénard convection arises as the warmer fluid ascends and the cooler fluid descends. A large-scale circulation of the bulk fluid emerges from the turbulent flow as the system

exceeds a threshold of external forcing [16–22]. The forcing intensity is characterized by the dimensionless Rayleigh number [23], $Ra = \alpha g \Delta T H^3 / \nu \kappa$, where g is the acceleration due to gravity, ΔT is the temperature difference between bottom and top, H is the depth of the fluid, and α , κ , and ν are the thermal expansion coefficient, the thermal diffusivity, and the kinematic viscosity of the fluid, respectively. The threshold Rayleigh number for a large-scale flow to appear is on the order of 10^7 [17,24]. Near the top and bottom plates, thin thermal boundary layers exist, within which convection is suppressed by the no-slip condition at the fixed plates and heat goes through by conduction. The thickness of the thermal

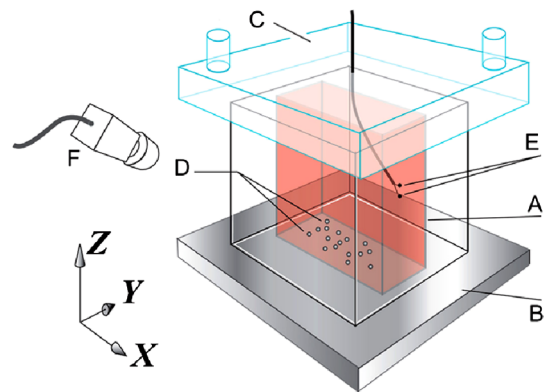


FIG. 1 (color online). A thermal convection cell (A) is inside of another box containing the same fluid and subject to the same cooling (C) and heating (B), so that box A is well insulated at all vertical walls. Nylon spheres (D) can roll freely on the smooth, mirror-quality bottom of A, as they are entrained by the convecting fluid. A pair of vertically separated thermistors (E) measures the bulk temperature and flow velocity through the cross-correlation between the two signals. Conformal mapping of the images taken by a video camera (F) produces top-viewed patterns of the spheres.

boundary layer λ_{th} is observed to have different scaling dependencies on the Rayleigh and Prandtl numbers ($Pr = \nu/\kappa$) in various regimes, as summarized by Grossmann and Lohse [5,25]. In the regime of our experiment, $Ra \sim 10^{8-9}$ and $1 < Pr < 10^2$, the scaling relationship is given by the measurement of Ashkenazi and Steinberg [26], $\lambda_{th}/H = 2.3 Ra^{-0.3} Pr^{0.2}$.

As shown in Fig. 1, a Rayleigh-Bénard convection cell of $20 \times 18.4 \times 7.6$ cm ($H \times L \times W$), containing a water-glycerol mixture ($\rho = 1.115$ g/ml), is heated from below by a dc electric heater and cooled at its top with a water circulator. The relatively smaller width (W) of the cell allows only two possible large-scale circulations to exist at high Rayleigh numbers ($Ra > 10^7$): a clockwise circulation or a counterclockwise one (from the perspective of the camera) that occupies the entire cell.

The freely moving objects introduced into the inner convection cell are nylon spheres, a few millimeters in diameter (d) and 2% denser ($\rho' = 1.134 \pm 0.002$ g/cm³) than the fluid. A large number of the spheres— N , on the order of a few hundred—form a single loose layer at the bottom. Each sphere experiences Stokesian drag from the convective flow, $F_{drag} \sim 3\pi\rho\nu dU$, on the order of a few hundredths of a dyne, given d and the speed of the convecting flow U . Because of the near Boussinesq nature [27] of the convection system—the thermal properties (besides density) of the fluid do not change with temperature—it can be regarded to have top-bottom symmetry. This experiment hence represents also the situation when many free-moving bodies float above and interact with a thermally convecting fluid beneath.

In the absence of the spheres, the large-scale circulation of either direction is stable up to a time scale of ~ 40 h. Beyond this time scale, its direction can flip spontaneously in a random fashion. This is consistent with earlier observations with a cylindrical cell as the rare cessation events took place [8,9], and such flow reversals are regarded as a result of hydrodynamical fluctuations overcoming a potential barrier that separates the possible states [28].

Having added the spheres to the convection cell, we find a drastic acceleration of these flow reversal events. Driven by the reversing circulation, the spheres pack and unpack cyclically. Shown in Fig. 2, the spheres are entrained by the flow and assemble at one end of the cell bottom [Figs. 2(a) and 2(c)]. This aggregation is progressive, often occurring by one sphere at a time or in small clusters. Typical packing patterns include thin strips of square lattice aligned with the sidewalls and small patches of hexagonal patterns near the interior. These patches are pieced together randomly as they evolve in time. As the flow reverses direction, the spheres become unpacked [Figs. 2(b) and 2(d)]. Figures 3(a) and 3(b) show that unpacking of the aggregate starts soon after the circulation reverses direction. As shown in Fig. 2(e), flow reversal happens only after the majority of spheres have collected on one side.

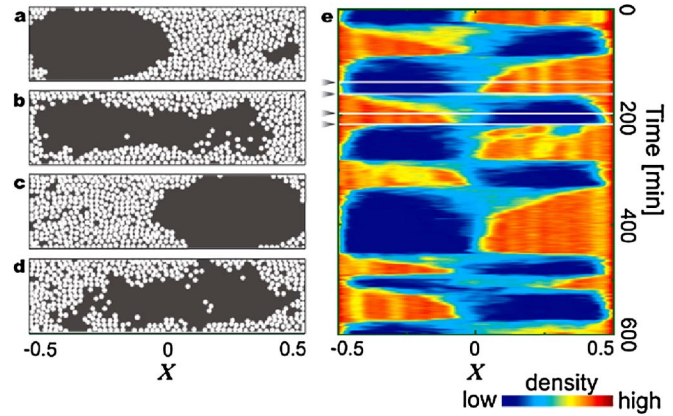


FIG. 2 (color online). Interaction between 426 spheres of diameter 3.2 mm and the convective fluid at $Ra = 3.2 \times 10^9$. (a)–(d) Four successive snapshots of the spheres during one cycle of two adjacent reversals. Instances (a),(c) show relatively dense packing and (b),(d) show the transient period as the aggregate is unpacked. Each of the snapshots is averaged along the short side of the convection cell to obtain a one-dimensional density profile. The evolution of such profiles (e) demonstrates cyclic packing and unpacking of the mobile spheres, with the four horizontal lines corresponding to the instances shown on the left.

Even though these flow reversals take place with randomness, an average reversal interval can be well-defined at each experimental condition (Ra and N).

The migration of an individual sphere takes up to a few tens of seconds, which is 2–5 times the duration needed for the circulation to flow across the bottom. However, it can take considerable time for a dense packing to assemble. Jamming of spheres during the packing phase often yields vacancies [e.g., the one near the right end of Fig. 2(a)]. The extent and location of these vacancies fluctuate in time and are likely to be filled before the next reversal. It is conceivable that the process of achieving dense packing is the main source of randomness in the timing of flow reversal.

The longest time scale in the oscillation is apparently that between flow reversals. Once the circulation changes direction, it achieves its full strength in a much shorter time scale, typically within a few flow circulations [Fig. 3(a)]. Because of the coupling with the free-moving spheres, relatively stable large-scale circulations are interrupted by abrupt flow reversal events and followed by the slow and accumulative aggregation of free-moving bodies. Figure 3(b) shows the correlation between the flow velocity and the position of the aggregate as a whole.

The spheres play an important role in inducing the circulation to reverse. The reversing frequency depends on the effectiveness of the perturbation introduced by the spheres. Figure 3(c) illustrates the feedback mechanism that is likely to operate in the coupled system of solid and fluid. Previously, we have shown that a solid boundary of similar material and thickness reduces the local heat transfer by a factor of order 10, because it prohibits local

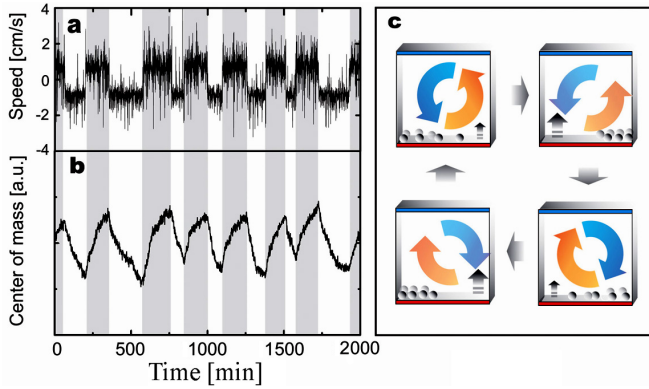


FIG. 3 (color online). Correlation between the large-scale circulation and the collection of the spheres. Here, $N = 510$, $d = 3.2$ mm, and $Ra = 1.8 \times 10^9$. (a) Time series of the circulation velocity, switching between two states. (b) The center of mass of all spheres varies in phase with the two circulations (white bands for clockwise and gray bands for counterclockwise). Illustration (c) shows the interplay between the large-scale circulation and the spheres. Once packed, the spheres collectively counteract the circulation by suppressing the local heat flux (stronger heat flux shown as vertical arrow). The large-scale flow eventually reverses direction. The new circulation unpacks the spheres and drives them to the other side of the cell, where they are reassembled. Once initiated, this process repeats.

convective heat transfer [13,15]. This effect is similar to the thermal blanketing effect of a solid boundary studied in geophysical contexts [29,30]. In this experiment, the precise heat-transfer contrast between a sphere-packed area and an unpacked area depends on the detailed packing configuration. For a typical random packing, we estimate that such contrast is on the order of 3–5, based on the volume occupied by the spheres compared with a solid block. Collectively, the aggregate of spheres acts as a thermal blanket that reduces the local heat flux from the bottom plate. The relatively enhanced local heat influx at the unoccupied areas eventually overturns the existing large-scale circulation.

To modify the amplitude and nature of the perturbation to the system, we use different sizes of spheres, vary the coverage ratio by adjusting the number of spheres, and also vary Ra . As we change the boundary layer thickness by varying the Ra , we find that there is a minimal flow reversal interval when $\lambda_{th} \sim d/2$, as shown in Fig. 4(a). We conjecture that the thermal blanketing effect of an individual sphere is affected by its area fraction at a height h from the bottom (the cross-section area at height h normalized by its maximum cross-section at height $d/2$), which is $\Gamma = 4(d-h)h/d^2$, where $h < d$. When $h = d/2$, this expression takes its maximum value. Our observation hence suggests that when the sphere radius ($d/2$) is close to λ_{th} , the activity at the edge of the thermal boundary layer, the most active region in a thermally convecting fluid [31], is most efficiently suppressed.

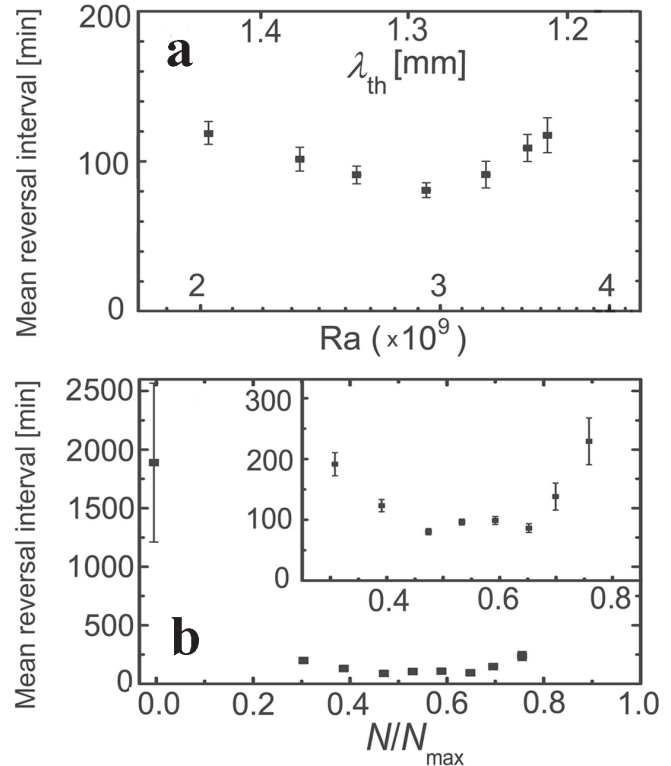


FIG. 4. The Rayleigh number and the number of free spheres are varied. (a) The circulation reversal intervals as a function of the Rayleigh number when $d = 3.2$ mm and $N = 365$. An oscillation with shortest reversal interval is obtained when the thickness of the thermal boundary layer λ_{th} is comparable to the radius ($d/2$) of the spheres. (b) At $Ra = 3.1 \times 10^9$ and $d = 3.2$ mm, the dependence of the reversal interval on the number of spheres. N_{max} (~ 840) is the number of spheres needed to fill up the bottom with random packing [32]. The inset shows the zoom-in detail of the data at $N \sim N_{max}/2$.

We notice that the radius of the spheres ($d/2 = 1.6$ mm) is about 23% greater than the thickness of the thermal boundary layer ($\lambda_{th} = 1.3$ mm) when the maximum reversal rate is observed [Fig. 4(a)]. We explain below this mismatch and show that the heat blocking effect is most effective when λ_{th} is somewhat smaller than $d/2$.

Nylon spheres have nearly the same heat diffusivity as the fluid. For an individual sphere, the vertical heat flux has to pass through both the solid sphere (thickness of order $d/2$) and a thermal boundary layer (thickness of order λ_{th}) that covers on the top of the sphere. The contrast between the heat fluxes with (j) and without (j_0) the spheres can be characterized by number $C = (j_0 - j)/j_0 = d/(2\lambda_{th} + d)$, which ranges from 0 to 1 as for no heat blocking to ideal blocking. The effective thermal blanketing factor Θ is the combination (product) of the vertical heat contrast C and the area fraction Γ taken by the spheres, and $\Theta = C\Gamma = 4\lambda_{th}(d - \lambda_{th})/d(2\lambda_{th} + d)$. When $\lambda_{th} = d(\sqrt{3} - 1)/2 = 1.2$ mm, factor Θ takes its maximum value and the heat blocking effect is most efficient. This

number is more consistent with our experimental observation. Indeed, the above argument serves only as a guide to better understand the heat blanketing effect of the spheres; it does not take into account the spheres' geometry and the detailed packing patterns.

Moreover, the number of spheres affects the reversal rate; it is greatest when the spheres cover about half of the bottom plate [Fig. 4(b)]. At this coverage, the spheres can create the highest contrast in heat flux at the bottom. With either a smaller or greater number of spheres, the bottom becomes geometrically more homogeneous and the heat contrast is reduced. Further, with more spheres present in the system, the suppressed mobility of spheres due to crowding also leads to longer reversal interval.

We have shown that a self-sustained, reorganizing state emerges as large-scale feedback (between many free bodies and the surrounding fluid) overrides chaotic features intrinsic to a turbulent flow. Our observation shows that the freely moving bodies introduced here do not destroy the existing coherent fluid structures, nor do they elicit more complex patterns in the system, but rather they provoke frequent switching between the two circulatory states. These free bodies, to some degree, are organized cyclically through passive response to the fluid; indeed, the collection of many free boundaries in our experiment behaves as a single deformable mass. We expect yet richer dynamics to occur if a similar study is conducted in cells with much greater aspect ratios, where several large-scale circulation regions and dynamical states may coexist.

We thank A. Libchaber, M. Shelley, S. Spagnolie, T. Bringley, J. Percus, and J.-Q. Zhong for helpful discussions. This work is supported in part by the Department of Energy (Grant No. DE-FG0288ER25053).

*jun@cims.nyu.edu

- [1] L. P. Kadanoff, *Phys. Today* **54**, No. 8, 34 (2001).
- [2] M. C. Cross and P. C. Hohenberg, *Rev. Mod. Phys.* **65**, 851 (1993).
- [3] J. Maurer and A. Libchaber, *J. Phys. (Paris), Lett.* **41**, L515 (1980).
- [4] M. H. Jensen *et al.*, *Phys. Rev. Lett.* **55**, 2798 (1985).

- [5] S. Grossmann and D. Lohse, *Phys. Rev. Lett.* **86**, 3316 (2001).
- [6] J. J. Niemela *et al.*, *Nature (London)* **404**, 837 (2000).
- [7] J. A. Glazier *et al.*, *Nature (London)* **398**, 307 (1999).
- [8] E. Brown, A. Nikolaenko, and G. Ahlers, *Phys. Rev. Lett.* **95**, 084503 (2005).
- [9] H.-D. Xi, Q. Zhou, and K.-Q. Xia, *Phys. Rev. E* **73**, 056312 (2006).
- [10] J. Crank, *Free and Moving Boundary Problems* (Clarendon Press, Oxford, 1984).
- [11] S. Vogel, *Life in Moving Fluids: The Physical Biology of Flow* (Princeton Press, Princeton, NJ, 1994).
- [12] J. A. Whitehead, *Phys. Earth Planet. Inter.* **5**, 199 (1972).
- [13] J. Zhang and A. Libchaber, *Phys. Rev. Lett.* **84**, 4361 (2000).
- [14] E. N. Popova and P. G. Frik, *Fluid Dyn.* **38**, 862 (2003).
- [15] J.-Q. Zhong and J. Zhang, *Phys. Fluids* **17**, 115105 (2005); *Phys. Rev. E* **75**, 055301(R) (2007).
- [16] W. V. R. Malkus, *Proc. R. Soc. A* **225**, 185 (1954).
- [17] R. Krishnamurti and L. N. Howard, *Proc. Natl. Acad. Sci. U.S.A.* **78**, 1981 (1981).
- [18] M. Sano, X. Z. Wu, and A. Libchaber, *Phys. Rev. A* **40**, 6421 (1989).
- [19] B. Castaing *et al.*, *J. Fluid Mech.* **204**, 1 (1989).
- [20] S. Ciliberto, S. Cioni, and C. Laroche, *Phys. Rev. E* **54**, R5901 (1996).
- [21] X.-L. Qiu and P. Tong, *Phys. Rev. E* **64**, 036304 (2001).
- [22] Y. Tsuji *et al.*, *Phys. Rev. Lett.* **94**, 034501 (2005).
- [23] Lord Rayleigh, *Philos. Mag.* **32**, 529 (1916).
- [24] T. Hartlep, A. Tilgner, and F. H. Busse, *Phys. Rev. Lett.* **91**, 064501 (2003).
- [25] S. Grossmann and D. Lohse, *J. Fluid Mech.* **407**, 27 (2000).
- [26] S. Ashkenazi and V. Steinberg, *Phys. Rev. Lett.* **83**, 3641 (1999).
- [27] J. Boussinesq, *Theorie Analytique de la Chaleur* (Gauthier-Villars, Paris, 1903), Vol. 2.
- [28] K. R. Sreenivasan, A. Bershadskii, and J. J. Niemela, *Phys. Rev. E* **65**, 056306 (2002).
- [29] F. H. Busse, *Geophys. J. R. Astron. Soc.* **52**, 1 (1978).
- [30] C. Grigné and S. Labrosse, *Geophys. Res. Lett.* **28**, 2707 (2001).
- [31] A. Belmonte, A. Tilgner, and A. Libchaber, *Phys. Rev. Lett.* **70**, 4067 (1993).
- [32] E. L. Hinrichsen, J. Feder, and T. Jøssang, *Phys. Rev. A* **41**, 4199 (1990).